# Dynamic Penetration Test with Measuring Shear Wave Velocity

Shunichi Sawada
*OYO corporation, Saitama, Japan, sawada-shun@oyonet.oyo.co.jp*

**ABSTRACT:** Piezo Drive Cone (after called “PDC”), which is a dynamic penetration test with pore water pressure measurement, was developed to evaluate the ground liquefaction assessment during earthquake more easily and economically. However, PDC cannot estimate soil classification in the soil layer shallower than the groundwater level. Because the pore water pressure response cannot be measured in unsaturated ground. The soil classification is estimated from the pore water pressure response at the time of dynamic penetration. In recent years, there has been a demand for evaluation of liquefaction assessment in a wider ground environment, and there is a need for a new investigation technique capable of using dynamic penetration resistance ($N_d$ value) and soil classification even upper the groundwater level. In order to respond to the request for evaluation of liquefaction assessment in the soil layer shallower than the groundwater level, I developed a dynamic penetration test with the shear wave velocity ($V_S$) of the ground which is named “Seismic PDC”. This report introduces the outline of “Seismic PDC” which can estimate soil classification even in unsaturated soil layer and can perform liquefaction assessment with method of unsaturated soil classification.

**Keywords:** Liquefaction assessment, Soil classification, Shear wave velocity, Dynamic penetration, Sounding,

## *1. Introduction*

The conventional ground investigation method has been standardized by the standard penetration test (SPT) to measure $N$ value (STP-$N$ value) using the rotary type machine boring in Japan. The rotary type machine boring with muddy water circulation is possible to drilling as various grounds from soft ground to hard ground which becomes the supporting soil layer of the building. However, it is said that ground investigation by machine boring with muddy water circulation requires sufficient space and time and expense to investigate. Therefore the ground investigation using machine boring inteval planned is far from 100 m or more. And in the depth distribution as well, there is only one point of information at every depth of 1 m by SPT. Because of that it has been pointed out that the resolution of the ground information using SPT with machine boring to be obtain is not high. Therefore, other sounding equipements methods are interpolated and used. A commonly used sounding method is the Cone Penetration Test (CPT) that can continuously obtain information in the depth direction with static penetration [7]. Nevertheless, in the static penetration method, the excess pore water pressure generated by penetration quickly dissipates in sandy grounds with high permeability. So it is impossible to measure the undrained strength as the ground using static penetration tool like the CPT. Affter all, the undrained strength such as liquefaction strength cannot be determined using static penetration method [6]. On the other hand, the dynamic penetration sounding method like a Swedish Rum Sounding (SRS) that can measure the undrained strength of the ground as equivalent to SPT-$N$ value, but also has a weak point that cannot identify the soil classification.

The seismic PDC has been developed for the purpose of reinforcing the weak point of the conventional. PDC was developed to evaluate the liquefaction assessment of the ground and measures the excess pore water pressure generated around the tip cone immediately after dynamic penetration, estimates the fines contents $F_C$ and identifies the soil classification [4]. However, based on the principle of estimating soil classification by measuring the excess pore water pressure response, it is impossible to estimate soil classification in unsaturated soils that are below the groundwater level. Because the excess pore water pressure response cannot be accurately measured in unsaturated soils.

If only conventional liquefaction assessment is required, soil classification below the groundwater level is unnecessary. However, it would be a useful ground investigation method if it is possible to identify the soil classification below the groundwater level of the road embankment or the river bank using a sounding tool with functions of time shortening, mobility and economic advantages. On the other hand, in Urayasu City etc. in the 2011 Tohoku Region Pacific Offshore Earthquake, there are also indications that liquefaction damage has spread due to the aftershocks occurred 30 minutes after the main shock, and according to the groundwater level rising due to ground liquefaction at the time of the mainshock. It is also pointed out that it is necessary to judge whether or not to liquefy unsaturated ground.

Based on these finding points, this report introduces Seismic PDC, a test method for improving PDC to be an investigation method capable of identifying soil classification even under unsaturated soils that are below the groundwater level.

## *2. Outline of Seismic PDC system*

As the title indicates, the introduced seismic PDC is a "Dynamic penetration test with measuring shear wave velocity", and shear wave vibration generated at the location of cone tip at the time of dynamic penetration is measured with a geophone disposed on the ground surface.

As a shear wave velocity measurement, it corresponds to the "uphole method". "Uphole method" is measured with geophones placed on the ground surface and the oscillation source by dynamic penetrating at the cone tip. On the other hand, "downhole method" often used in ground survey is blowing the board on the ground surface and measurement geophones located into the borehole. Both are the measurement of the oscillation source and the receiving geophones in reverse arrangement.

Fig. 1. shows a system conceptual diagram of the seismic PDC. It is a specification that added triaxial components geophones which measure blowing vibrations at two or more places on the ground surface with the conventional PDC measurement system. The oscillation source of the shear wave is generated when the tip of the cone dynamic penetrates into the ground. The shear wave source gradually gets deeper with dynamic penetration, not only the distance is away from the geophone but also the incident angle changes.

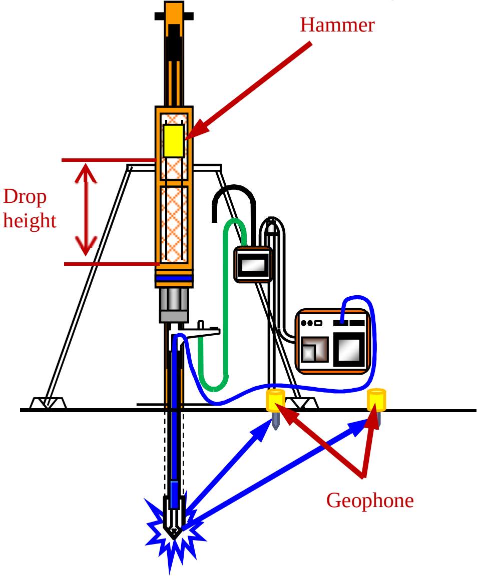

**Figure 1.** Conceptual diagram of the seismic PDC.

Also, Fig. 2. shows the radiation patterns of a) shear wave and b) compressional wave. The vertical shear wave velocity $V_{SV}$ and the compressional wave velocity $V_P$ in the longitudinal direction can be measured from the relation of the dynamic penetration of the cone tips. Vibrations of the vertical and the horizontal component are recorded by using the triaxial components velocity measurement type geophone installed on the ground surface with the vibration generated by vertical dynamic cone penetration at the bottom of the borehole.

From the relationship shown in Fig. 3., the amplitudes of the vibrations are obtained from the compressional wave $V_P$ and the shear wave vertical component $V_{SV}$ by Eq. (1).

$$V_P = V_V \csc\theta = V_H \sec\theta$$
$$V_{S_V} = V_V \cos\theta = V_H \sin\theta \qquad (1)$$

## 3. Relation between stiffness $V_s$ and strength N value

### 3.1. Relation between $V_S$ and N value

Fig. 4. shows the Imai and Tonouchi formula which is the relationship between SPT-*N* value and shear wave velocity $V_S$ in 1982 [1]. As you can see, it shows positive correlation. However, if you look closely from the

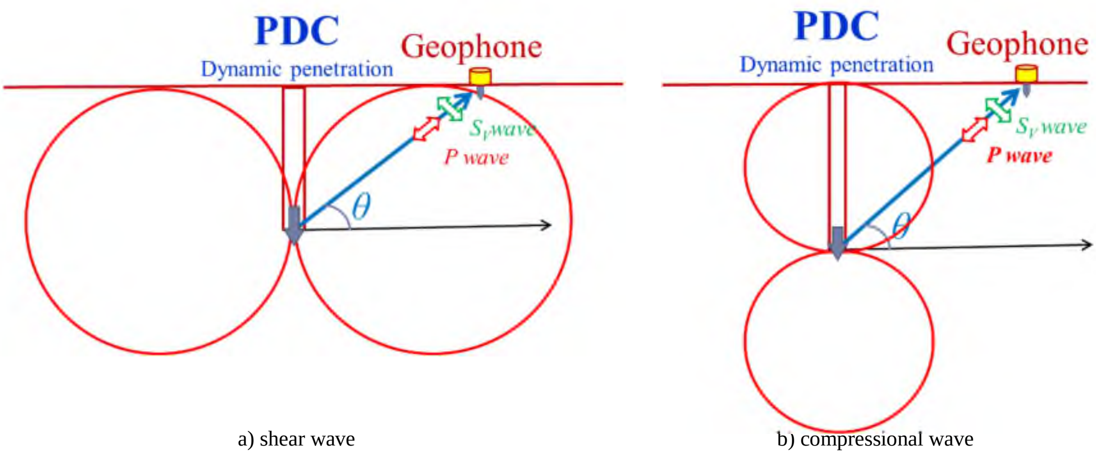

a) shear wave

b) compressional wave

**Figure 2.** the radiation patterns.

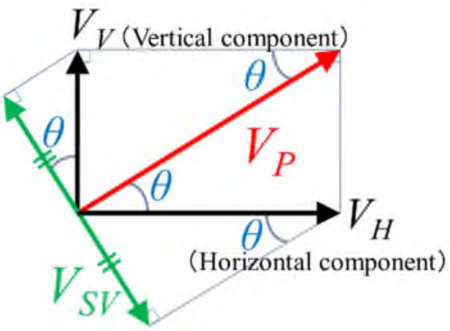

**Figure 3.** Amplitudes of the vibrations

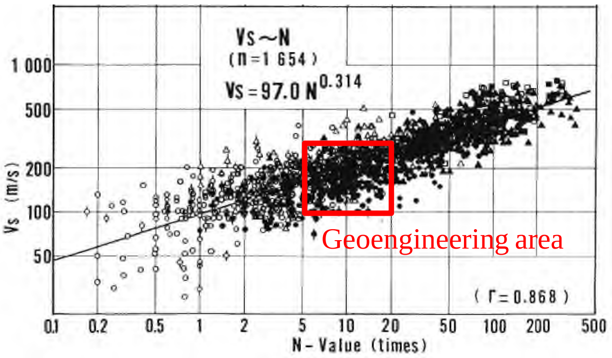

**Figure 4.** relational between *N* value and $V_S$

viewpoint of geotechnical engineering, the scale of *N* value is 0.1 to 500 and the shear wave velocity $V_S$ is 10 to over 2,000m/s. Furthermore, both axes are not linear scale but log scales. The range of $V_S$ used by geotechnical engineers who design for soft ground is 100m/s or more and less than 300m/s. At the same time, the range of *N* values is 5 to 20. Focusing on this range from the Fig. 4., there is no correlation between *N* value and $V_S$. Here, considers the physical relationship between *N* value and $V_S$. Fig. 5. shows the illustration of the relation between shear strain $\gamma$ and shear stress $\tau$ . Shear wave velocity $V_S$ has a relation of Eq.(2) using initial shear stiffness $G_0$ and soil mass $\rho$ as a ground physical property. $V_S$ is a characteristic showing initial shear stiffness.

$$G_0 = \rho \cdot V_s^{\,2} \tag{2}$$

On the other hand, *N* value indicates the ultimate strength of the ground. Of course the characteristics of stiffness and strength are different dimensions. Everyone knows that there is no clear relationship between stiffness and strength. In other words, everyone knows that even the same strength ground be able to have different stiffnesses. Even if *N* value is obtained, $V_S$ is not obtained, and even if $V_S$ is obtained, *N* value is not obtained.

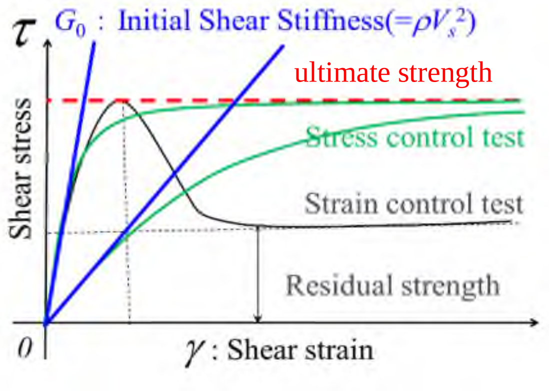

**Figure 5.** Schematic figure of stress versus strain.

## 3.2. Relation between N value and $V_S$ and coefficient α

Fig. 6. shows the relationship between SPT-*N* value and $V_S$ by the ground survay results using the latest technology obtained from site characterization in Urayasu City after the 2011 Tohoku Earthquake, Japan [2,5]. There is no positive correlation between SPT-*N* value and $V_S$. From these results, it is clear that the correlation between SPT-*N* value and $V_S$ is not remarkable in the range of ground materials handled by geotechnical engineers. Here is the expression of Eq. (3) written in the Specification for highway briges of Japan Road Association [3].

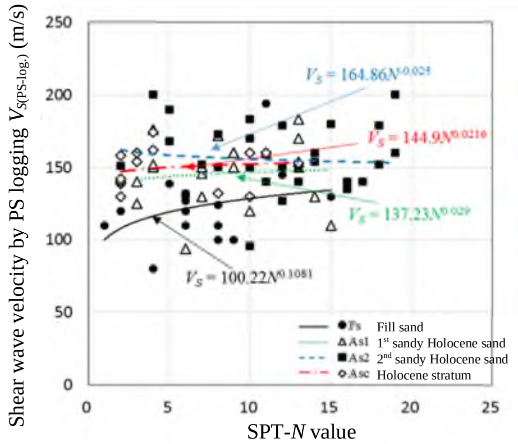

**Figure 6.** SPT-*N* value versus measured $V_S$.

*In case of clayey soil:*

$$\left.\begin{array}{l} V_{si} = 100N_i^{\,1/3} \quad (1 \le N_i \le 25) \\ \textit{In case of sandy soil:} \\ V_{si} = 80N_i^{\,1/3} \quad (1 \le N_i \le 50) \end{array}\right\} \tag{3}$$

Eq. (3) is a relational expression that $V_S$ value is obtained by multiplying ⅓ power of *N* value by coefficient *α*. Also, there is a relationship that the factor *α* is determined by the soil classification. Therefore, Fig. 7. shows the correlation between $N_1$ value which is converted by effective overburden pressure $\sigma'_v$ measured depth by Eq.(4) and $N_1$ value back calculated by the coefficient *α* determined using grouping ranged fines content $F_C$. It is recognized that there is a clear correlation between converted $N_1$ value and inversed $N_1$ value using $V_S$ if the fines content $F_C$ is clarified.

$$N_1 = 170\,N/(\sigma'_v + 70) \tag{4}$$

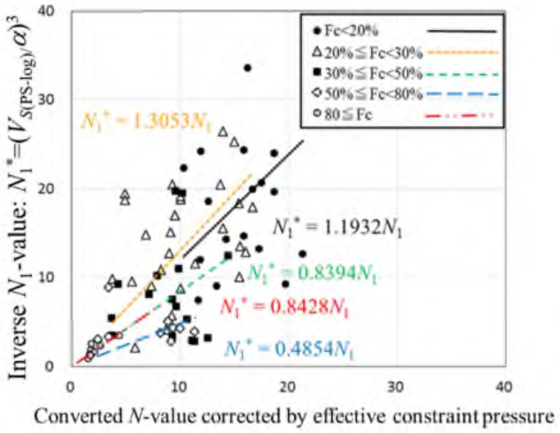

**Figure 7.** Correlation between measured and back calculated $N_1$ value.

## 3.3. Coefficient α and fines content $F_C$

Fig. 8. shows the coffecient *α* estimated by the Eq. (5) using the SPT-*N* value obtained and the shear wave

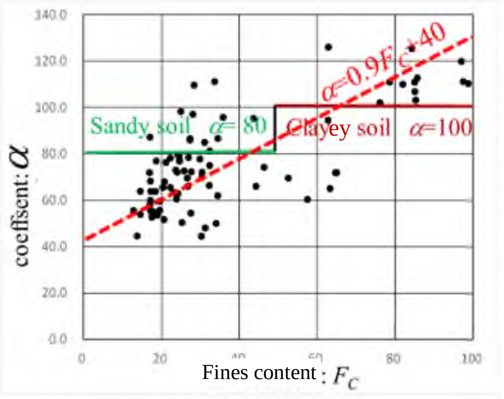

**Figure 8.** Correlation between $F_C$ and coefficient α.

velocity $V_S$ measured by the PS logging in the same borehole.

$$\alpha = V_s / N^{1/3} \quad (5)$$

From Fig. 8., a positive correlation is found between the coefficients $\alpha$ and $F_C$, and the relationship of Eq. (6) is estimated.

$$\alpha = 0.9F_C + 40 \quad (6)$$

### 3.4. Magic triangle

It was found that there was a coefficient $\alpha$ expressed by the fines content $F_C$ in relation to the shear wave velocity $V_S$ and the $N$ value. As a result, the magic triangle shown in Fig. 9. exists between the three elements, $V_S$, $N$ value and coefficient $\alpha$. These three elements are mutually influenced relationships, and if two of them are decided, the remaining one is naturally determined. In other words, if you know $N$ value and $V_S$, the fines content $F_C$ can be found through the coefficient $\alpha$. From this relationship, it is possible to estimate soil classification by measuring $N$ value and $V_S$ whether saturated or unsaturated soil.

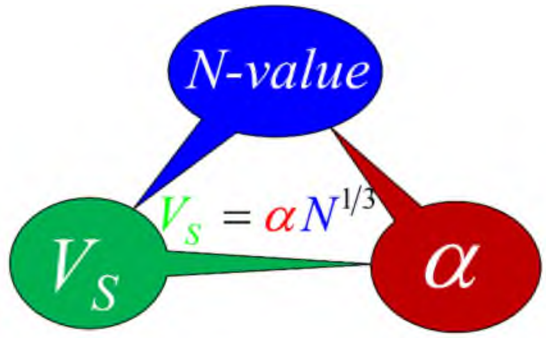

**Figure 9.** Magic triangle of three elements $N$ value, $V_S$ and coefficient $\alpha$.

## 4. Measurement experiment example using prototype testing tool

As prototype of Seismic PDC with geophone measurement was conducted at Inagi City in Ibaraki prefecture. The test equipment used at the field is the intelligent type PDC (after called “iPDC”) which measures the pore water pressure and the load at the cone tip using Swedish Ram Sounding (SRS) for the dynamic penetration device.

### 4.1. Prototype specification

Fig. 10. shows the photograph of triaxial components geophone used in the prototype Seismic PDC. Furthermore, recording trigger was used which was installed around the proximity sensor to trigger the iPDC recording.

Since the start of the recording is due to the impact of the anvil on the ground surface, the time lag from surface to the cone tip depth must be calculated using the iron compression wave velocity ($V_P$=6,000m/s) of the rod material. Geophone was a triaxal components (xyz) specification but adopts two components record of a horizontal component (x) in normal direction which is heading toward the center of the dynamic penetration device and a vertical component (z).

**Figure 10.** Photograph of four triaxal geophones.

Fig. 11. shows the recording waveform in vertical motion (z) using the geophone at the point where the horizontal distance is 10 m. And Fig. 11. shows the depth distribution of $N_d$ values by Seismic PDC and nearby SPT-$N$ values using conven-tional machine bouring. Soil classification can be performed by measuring the $N_d$ and $V_S$ values for each depth. From the recording results, it is to a depth 10m is substantially uniform sandy soil layer, further, fines content $F_C$ can be estimated to be about 30% to 40%. Although it is not systemized, an automatic calculation system will be built in the near future.

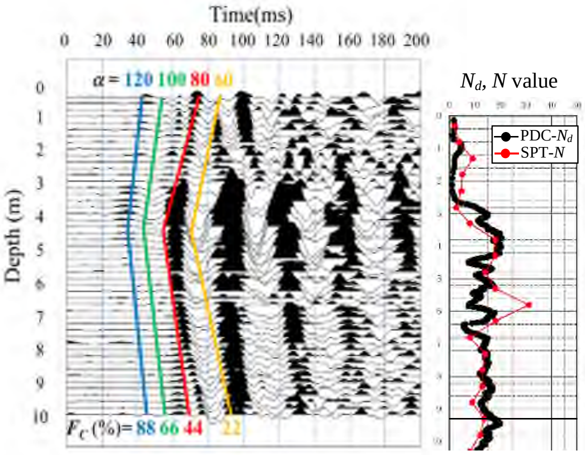

Horizontal distance=10m, Vertical

**Figure 11.** Recording waveform and $N_d$ value using SRS.

## 5. Case study of soil classification in surface wave exploration and dynamic penetration test

As a practical verification example of Seismic PDC, an example is shown in which soil classification is estimated from shear wave velocity $V_S$ obtained by surface wave exploration and $N_d$ value using PDC performed at the top of road embankment with deep groundwater level.

### 5.1. Verification results

Surface wave exploration was carried out at the top of the embankment made of loam material with tuff mixed with sand dunes on the foundation ground. Fig. 12. shows the results of the shear wave velocity $V_S$ as a two-dimensional sectional view using the surface wave exploration. As for the shear wave velocity in the part shallower than 5 m from the top of the embankment, the warm color of red to orange with $V_S$ value of 140 to 160 m/s is partially observed. The other part has a cold color from green to dark blue with a $V_S$ value of 170 to 270m/s. A total of 6 SRS and PDC were conducted. Six points are selected as three pairs. For the pair, select a nearby location that is shallower than 5m and has a significant difference in shear wave velocity. Fig. 13. shows the depth distribution of $N_d$ value at each point. The $N_d$ value shows a large value deeper than the old ground surface of the sand dune, and accurately shows the top of the sand dune layer. In addition, when the shear wave velocity $V_S$ and $N_d$ value are compared between adjacent pairs (for example, SRS No.1 and No.2, SRS No.3 and No.4, PDC No.5 and No.6) when the wave velocity $V_S$ is high, the $N_d$ value tends to increase.

## 6. Discussion

### 6.1. Depth distribution of shear wave velocity $V_S$ and $N_d$ value

Fig. 14. shows the depth distributions of $N_d$ value and shear wave velocity $V_S$. The $N_d$ values are reflects the strength of the ground at each depth except the part considered to be spot stones. On the other hand, the shear wave velocity obtained by surface wave exploration is an average value, and there is no precision equivalent to the $N_d$ value. At a depth of 3 m or more, no difference in shear wave velocity $V_S$ is observed except for an increase at SRS No. 4 point. The difference in accuracy between the SRS or PDC and the surface wave exploration results is remarkable.

### 6.2. Calculation of coefficient α and fines content $F_C$

The relationship between shear wave velocity $V_S$ and $N_d$ value (≈SPT-$N$ value) is shown in the following Eq. (3). According to the specifications for highway bridges, coefficient $\alpha$ is equal to 100 for clayly soil and equal to 80 for sandy soil. The data on which the coefficient $\alpha$ is based is proportional to the fines content $F_C$ and is expressed by the following Eq. (5) and Eq. (6). Then, the coefficients $\alpha$ and $F_C$ were calculated by applying the equations at 6 points on the road embankment. Fig. 15. shows the depth distribution of $\alpha$ and $F_C$. Although $\alpha$ varies in a wide range, it is more than 100, $F_C$ is also more than 50% and it is generally judged as "clayly soil".

### 6.3. The result of soil classification

Fig. 16. shows the depth distribution of calculated fines content $F_C$ at 6 points.

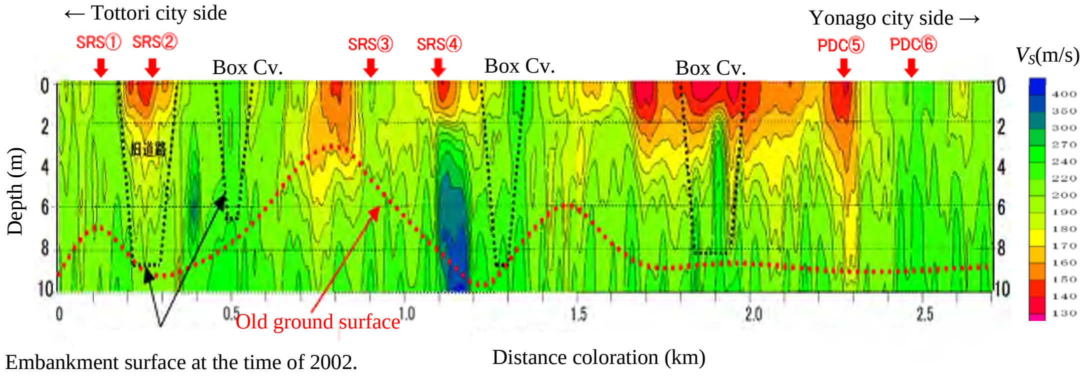

**Figure 12.** Cross section of shear wave velocity $V_S$ using surface wave exploration.

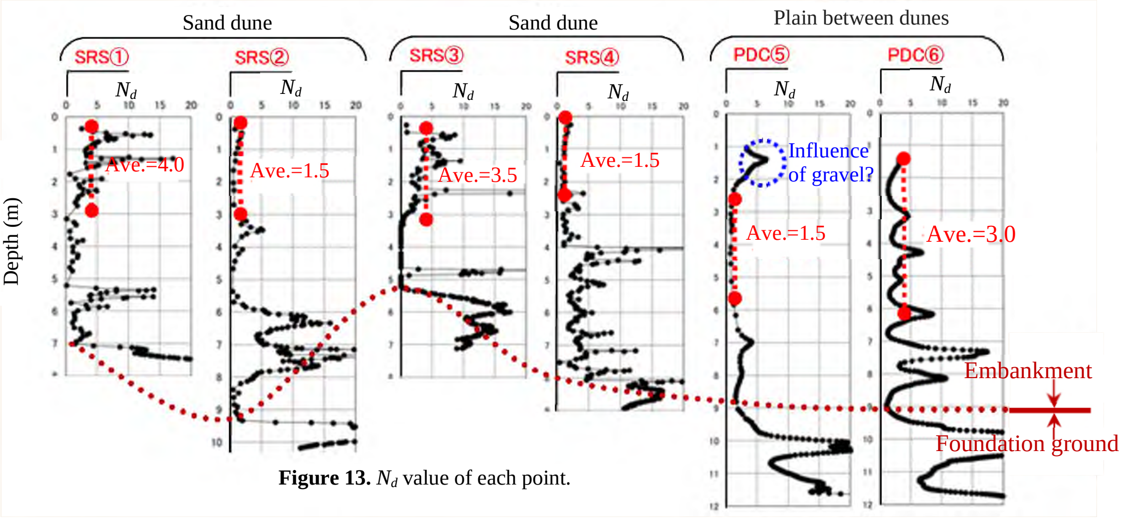

**Figure 13.** $N_d$ value of each point.

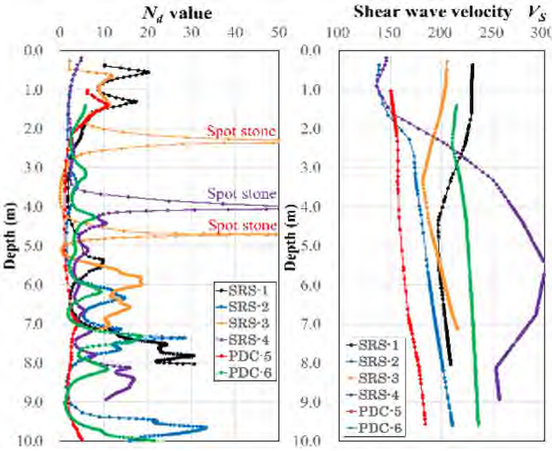

**Figure 14.** Depth distribution of $N$ value & $V_S$

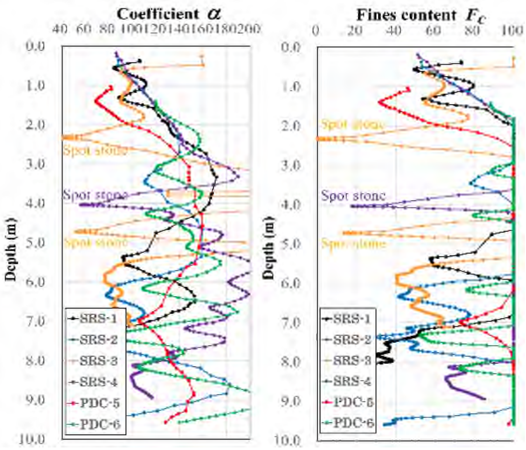

**Figure 15.** Depth distribution of α & $F_C$

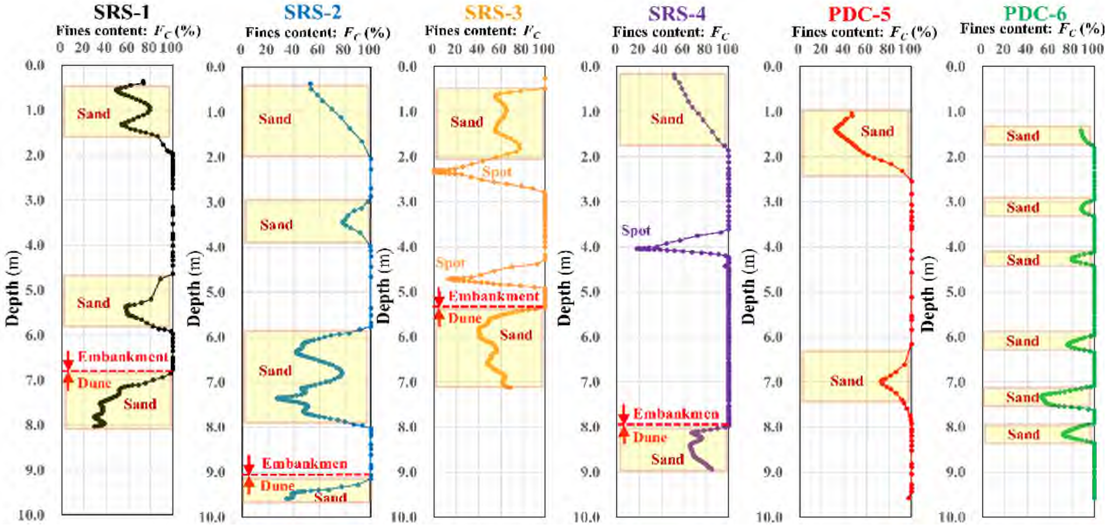

**Figure 16.** Results of soil classification

Although the results are part of a dune with a low fines content $F_C$, the fines content $F_C$ results show over 40%. From this result, in this report, when $F_C$ is equal to 100%, it is clayey soil, and when $F_C$ is less than 100%, it is identified as sandy soil and is shown in Fig. 16. Thus, the soil discrimination based on $V_S$ and $N_d$ values has not been able to be quantitatively estimation. However, estimation of qualitative claly soil or sandy soil is considered possible.

## 7. Afterword

CIM is recommended for the construction project as visualization of the ground. In Japan, in the construction business, we are promoting "i-Construction" to improve productivity at the construction site by utilizing ICT in every process from soil investigation and surveying to design, construction and maintenance. By introducing innovative technologies such as IoT and Artificial Intelligence (AI) on the construction field and utilizing three-dimensional data, we aim to create a new construction site with high productivity and attractive. Three-dimensional geotechnical information with increased resolution is also a major achievement target. Among them, development of an investigation method to obtain high-resolution ground information in a short time is also required. Correctly, Seismic PDC including iPDC can also be an important ground investigation tool. In this report, I could not introduce measurement examples as a single “Seismic PDC”. I will continue to collect data and continue to develop the advanced approaches and dissemination activities as investigation equipment tools.

## References

[1] Imai, T. and Tonouchi, K., 1982, Correlation of N-value with S-wave Velocity and Shear Modulus, Proceedings of the 2nd ESPT.

[2] Ishii, I., Hiradate, R., Towhata, I., Nakai, S., Sekiguchi, T., Sawada, S. and Hamada, Y., 2017, Liquefaction-induced damage to houses and site characterization in Urayasu City during the 2011 Tohoku Earthquake, Japan, Japanese Geotechnical Journal, Volume 12, Issue 1, pp. 91-107.

[3] Japan Road Association, 2012, Specifications for highway bridges part 5(seismic), p33.

[4] Sawada, S., 2009, Evaluation of differential settlement following liquefaction using Piezo Drive Cone, 17th International Conference on Geotechnical Engineering, Alexandria, Egypt, 1064-1067.

[5] Sawada, S., Hamada, Y., Ishii, I., Hiradate, R., Nakai, S., Sekiguchi, T. and Towhata, I, 2017, Liq-uefaction-induced damage to houses and site characterization in Urayasu City during the 2011 Tohoku Earthquake, Japan, proceeding of 3rd Inter -national Conference on Performance-based Design in Earthquake Geotechnical Engineering, Vancouver.

[6] Terzaghi, K. & R. B. Peck, 1948, *Standard penetration test method for relative density of cohensionless soils*. American Society for Testing and Materials, Philadelphia, D2049-69.

[7] Robertson, P.K., 1990, *Soil classification using the cone penetration test*, Canadian Geotechnical Journal, 27(1), 151-158.